Inorganic Chemistry

Article

pubs.acs.org/IC

Axial-Site Modifications of Paddlewheel Diruthenium(II, II) Complexes Supported by Hydrogen Bonding

Wataru Kosaka,[†] Naoto Yamamoto,[†] and Hitoshi Miyasaka*[,‡]

[†]Department of Chemistry, Division of Material Sciences, Graduate School of Natural Science and Technology, Kanazawa University, Kakuma-machi, Kanazawa 920-1192, Japan

[‡]Institute for Materials Research, Tohoku University, 2−1−1 Katahira, Aoba-ku, Sendai 980-8577, Japan

Supporting Information

ABSTRACT: The reactions of paddlewheel-type diruthenium(II, II) complexes, $[Ru_2^{II,II}(x\text{-}FPhCO_2)_4(THF)_2]$ (x-$FPhCO_2^-$ = x-fluorobenzoate with x- = o-, m-, p-), with 2,6-diaminopyridine (dapy) and 7-azaindole (azain) afford axially capped discrete compounds, $[Ru_2^{II,II}(x\text{-}FPhCO_2)_4(dapy)_2]$ (x = o-, **1**; m-, **2**; p-, **3**) and $[Ru_2^{II,II}(o\text{-}FPhCO_2)_4(azain)_2]$ (**4**), respectively. In these compounds, intramolecular hydrogen bonds are observed between NH_2 groups for **1**−**3** or imine NH groups for **4** and oxygen atoms of carboxylate groups. In addition, hydrogen bonds of $NH_2\cdots F$ are also observed for **1** and **4** with an o-positioned F atom on benzoate. This coordination mode, i.e., a dual bonding mode with σ-bonding and hydrogen bonding, should assist ligand coordination to the axial position of the $[Ru_2]$ unit. The Ru−N bond distance in **1**−**4** is shorter than that observed in related compounds reported previously. In a similar fashion, reactions with planar M^{II} dithiobiuret (dtb) complexes, $[M^{II}(dtb)_2]$ (M^{II} = Pd^{II} and Pt^{II}), were carried out. One-dimensional alternating chains, $[\{Ru_2^{II,II}(o\text{-}FPhCO_2)_4\}\{M^{II}(dtb)_2\}]$ (M^{II} = Pd^{II}, **5**; Pt^{II}, **6**), were obtained, in which the hydrogen-bonding modes of $NH_2\cdots O$ and $NH_2\cdots F$ are present, as expected. DFT calculations for the $[M^{II}(dtb)_2]$ unit revealed that the LUMO of $[M^{II}(dtb)_2]$ lies at −2.159 and −1.781 eV for M = Pd and Pt, respectively, which is much higher than HOMO energy at −4.184 eV calculated for $[Ru_2^{II,II}(o\text{-}FPhCO_2)(THF)_2]$, proving that the respective units are essentially electronically isolated in the chains.

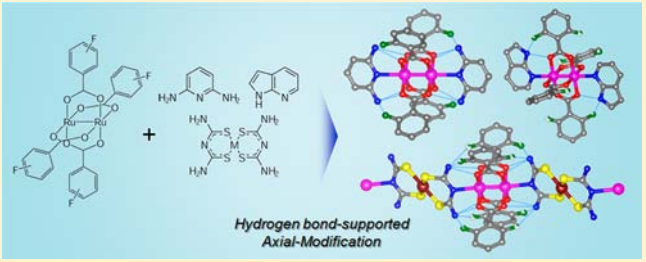

INTRODUCTION

The rational design of functional molecular assemblies and frameworks is a crucial issue in the field of solid-state chemistry and physics. Recently, we proposed a method to synthesize on-demand frameworks using a linear-type coordinating-acceptor building block (CABB) as "edge" of frameworks and a selectable coordinating-donor building block (CDBB) as "node" of frameworks.[1,2] In this way, the topology of constructed frameworks is modulated, dependent only on the shape and number of coordination sites of CDBB (i.e., node) used, as was systematized for finite cages by Stang et al.,[3] in cases where all coordination sites on CABB and CDBB are mutually saturated for bonding of frameworks (Figure 1). For the linear-type CABB, which is fixed in the above strategy, the family of paddlewheel-type dinuclear metal complexes ($[M_2]$) is useful for the purpose. The latter not only act as a good linear-type CABB,[4−6] but also provide electronic/magnetic functional centers involving metal−metal bonding,[7] flexible charge ordering,[8] redox activity,[7,9] and paramagnetism, based on the frontier orbitals.[7,10,11] Thus, the use of such a simple rigid core with selectable functionalities enables the simpler design of on-demand frameworks complete with functionalities.

The family of carboxylate-bridged paddlewheel-type diruthenium(II, II) complexes ($[Ru_2^{II,II}]$) is suitable for functional linear-type CABBs. Such complexes not only act as electron donors (D) to derive $[Ru_2^{II,III}]^+$ without significant structural change in reactions with adequate electron acceptors (A), but also contribute as a paramagnetic source with multiple spin states of S = 1, as well as $[Ru_2^{II,III}]^+$ with $S = {}^3/_2$,[10] due to the formation of Ru−Ru bonds with frontier orbitals.[7] The D/A assemblies with organic polycyano acceptors such as 7,7,8,8-tetracyano-p-quinodimethane (TCNQ) and N,N'-dicyanoquinodiimine (DCNQI) have demonstrated electron-transfer-driven magnetic ordering and electron transport properties in D/A frameworks such as one-dimensional (*1-D*; the dimensionality of the lattice, *1-D*, *2-D*, and *3-D*, is hereafter written in italics to distinguish it from "D" as donor) ladder-type chains,[12,13] *1-D* linear chains,[14] *2-D* networks,[15−19] and *3-D* infinite networks,[20,21] well organized by the concept mentioned above (see Figure 1).[2] Meanwhile, the bonding affinity at the axial sites of $[Ru_2^{II,II}]$ is selective, rather disadvantageous for ligands/CDBBs with a weak donation such as neutral TCNQ and DCNQI, where the assembly reactions with ligands/CDBBs should, therefore, be well controlled to exclude competing ligands such as solvents capable of coordinating from reaction media. To obtain a more flexible organization at the axial sites of the $[Ru_2^{II,II}]$ unit,

Received: April 29, 2013
Published: August 20, 2013

dx.doi.org/10.1021/ic401030r | *Inorg. Chem.* 2013, 52, 9908−9914

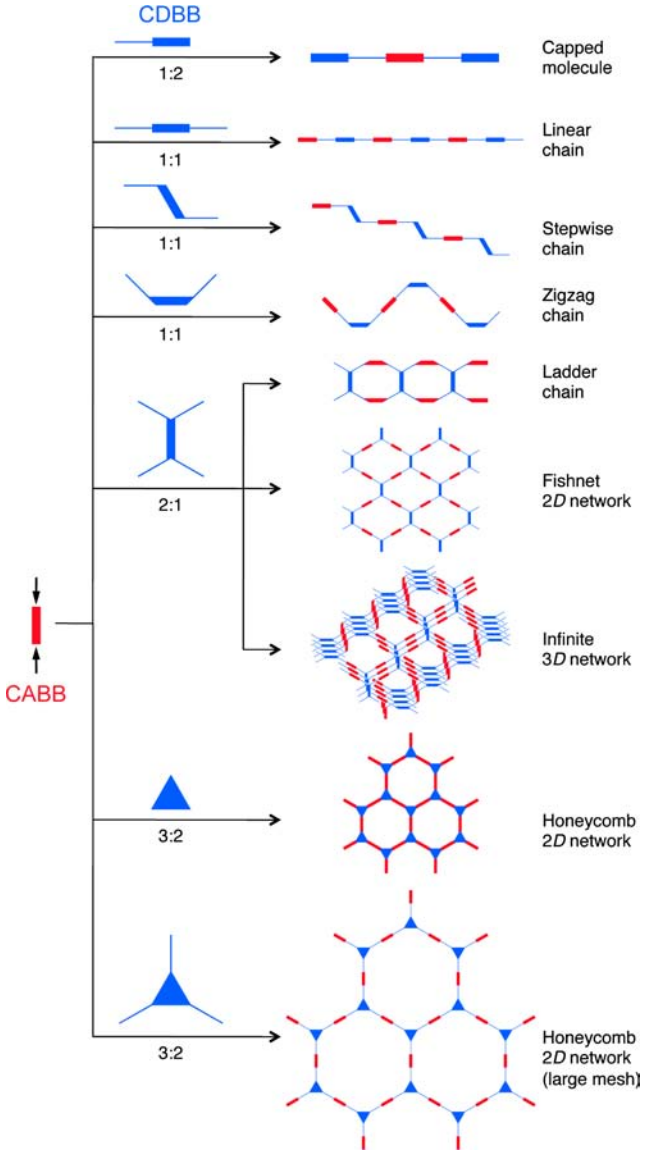

Figure 1. Expected structural topologies constructed by the combination of a linear-type CABB (red) and various types of CDBB (blue) following the rule that all coordination sites of building blocks are saturated for bonding (i.e., without vacant sites).

hydrogen bonding, in addition to the general covalent bond, is an efficient support, i.e., forming a dual bonding manner. In fact, several $[M_2]$ complexes, in which hydrogen bonding is involved, have already been discussed,[22,23] and a unique *1-D* alternating chain with $[Rh_2^{II,II}]$ and $[Ni(bpbg)_2]$ (bpbg = biphenylbiguanide) has been synthesized,[24] although the instance for multidimensional networks is limited in this case.

Here we used hydrogen bonding to create assemblies with $[Ru_2^{II,II}]$ units. Discrete molecules axially capped by 2,6-diaminopyridine (dapy) and 7-azaindole (azain), $[Ru_2^{II,II}(x\text{-}FPhCO_2)_4(dapy)_2]$ (x = *o-*, **1**; *m-*, **2**; and *p-*, **3**) and $[Ru_2^{II,II}(o\text{-}FPhCO_2)_4(azain)_2]$ (**4**), and *1-D* alternating chains with planar M^{II} dithiobiuret (dtb) complexes $[M^{II}(dtb)_2]$ (M^{II} = Pd^{II}, Pt^{II}), $[\{Ru_2^{II,II}(o\text{-}FPhCO_2)_4\}\{M^{II}(dtb)_2\}]$ (M^{II} = Pd^{II}, **5**; Pt^{II}, **6**), are reported.

RESULTS AND DISCUSSION

Synthesis and Characterization of Discrete Molecules 1−4. The reaction of $[Ru_2^{II,II}(x\text{-}FPhCO_2)_4(THF)_2]$ (x = *o-*, *m-*, *p-*) with excess dapy or azain (1:4 mol ratio) leads to the formation of discrete paddlewheel-type Ru dimers axially capped by the corresponding pyridine derivatives: $[Ru_2^{II,II}(x\text{-}FPhCO_2)_4(L)_2]$ (L = dapy, x = *o-*, **1**; *m-*, **2**; *p-*, **3**; L = azain, x = *o-*, **4**). IR spectra of **1**−**3** show two N−H stretching peaks in the range 3370−3480 cm^{-1}, which are blue-shifted compared to those for dapy (3308 and 3391 cm^{-1}). An IR spectrum of **4** shows one N−H stretching peak at 3333 cm^{-1}, similarly blue-shifted compared to that for azain (3123 cm^{-1}). Meanwhile, the peak positions of symmetric and antisymmetric C═O stretching vibrations are unchanged after the addition of pyridine derivatives. In powder reflection spectra of **1**−**4**, no specific charge transfer between $[Ru_2]$ unit and capping ligand is observed (Figure S1).

Structures of 1−4 and Description on Hydrogen Bonding. The structures of **1**−**4** were determined by single-crystal X-ray diffraction. Their crystallographic data, selected bond lengths and angles, and hydrogen bond distances are summarized in Tables S1, S2, and S3, respectively.

All compounds have an identical motif: a discrete Ru dimer axially capped by the corresponding pyridine derivatives. Compounds **1**, **2**, and **4** crystallize in the triclinic $P\bar{1}$ space group, where **1** and **4**, respectively, have two crystallographically unique $[Ru_2]$ units (Z = 2), and **3** crystallizes in the monoclinic $P2_1/c$ with Z = 4 (Figure 2 and S2 for another unit in **1** and **4**). For each unit in **1**, **2**, and **4**, an inversion center is located at the midpoint of the Ru−Ru bond, forming a centrosymmetric $[Ru_2(x\text{-}FPhCO_2)_4(L)_2]$ molecule; thus the half set of respective units forms an asymmetric unit, whereas all atoms of the formula unit were determined as an asymmetric unit for **3** (Z = 4). The Ru−Ru length is in the range 2.28−2.30 Å, slightly longer than that for $[Ru_2(x\text{-}FPhCO_2)_4(THF)_2]$ (2.2669(7) Å for x = *o-*, 2.2691(9) Å for *m-*, 2.2677(3) Å for *p-*):[9] when the Ru−N bond is strengthened, the Ru−Ru bond in general tends to lengthen. The average Ru−O_{eq} length (O_{eq} = carboxylate oxygen atoms) is typical for $[Ru_2^{II,II}]$ species (Table S2), because the Ru−O_{eq} lengths in the $[Ru_2^{II,II}]$ and $[Ru_2^{II,III}]^+$ complexes are generally found in the ranges 2.06−2.08 Å and 2.02−2.03 Å, respectively.[7,9,14] The Ru−N length in the quasilinear Ru−Ru−N linkage is in the range 2.32−2.44 Å, which tends to be slightly shorter than N-capped $[Ru_2^{II,II}]$ complexes with no hydrogen bonding reported previously, e.g., $[Ru_2(CF_3CO_2)_4(phz)]$ (phz = phenazine; 2.425(2) Å),[25] $[Ru_2(2,3,5,6\text{-}F_4PhCO_2)_4(acridine)_2]$ (2.450 Å),[26] and $[Ru_2(p\text{-}FPhCO_2)_4(phz)]$ (2.450(7) Å).[27] Except for one unit in **4** with ψ = 8.6° (vide infra), the two L planes at the axial positions almost bisect the paddlewheel arrangement, as similarly found in the phz-bridged $[Ru_2^{II,II}]$ chain $[Ru_2^{II,II}(CF_3CO_2)_4(phz)]$,[25] where a dihedral angle ψ, which is defined by an angle between L plane versus the O1−O2−O1*−O2* and/or O5−O6−O5**−O6** planes (see inset figure in Table S2), is found with ca. 45−50°. This configuration enables hydrogen bonding between one amino group on L and two oxygen atoms of the bridging carboxylate groups with N···O distances in the range 2.8−3.4 Å (only one unit in **4** has a one-site hydrogen bonding mode; see Figure 2d) (Figures 2 and S2, and Table S3). The position of amino groups in dapy and imino groups of azain also enables the formation of hydrogen bonds with fluorine groups of the *o*-FPh moiety, so only in **1** and **4**, with N···F

dx.doi.org/10.1021/ic401030r | Inorg. Chem. 2013, 52, 9908−9914

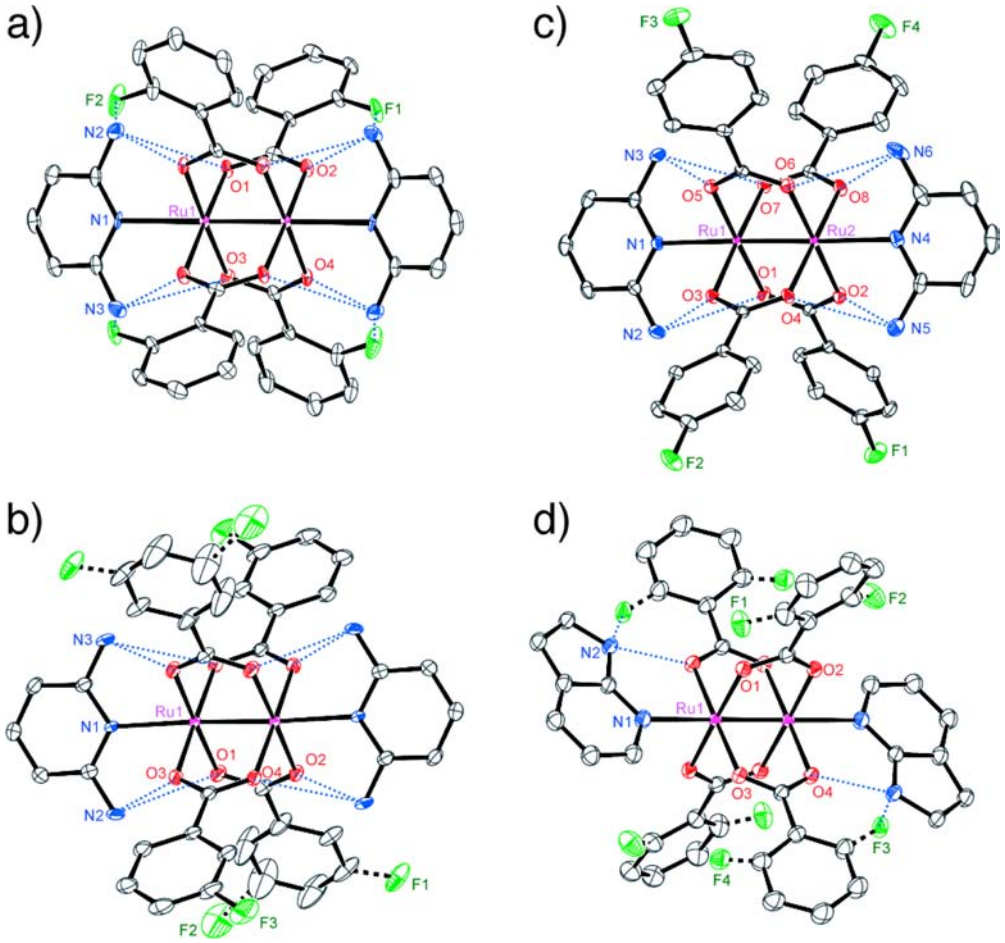

Figure 2. Thermal ellipsoid plots (50% probability) showing the formula unit for one unit of **1** (a), **2** (b), **3** (c), and one unit of **4** (d) (another unit for **1** and **4** is given in Figure S2), where atoms of N, O, C, F, and Ru are represented in colors of blue, red, gray, green, and purple, respectively, and blue dotted lines represent hydrogen bonds. Hydrogen atoms and crystallization solvents were omitted for clarity.

distances in the range 2.90−3.54 Å. An interesting aspect is that the average dihedral angle, θ_{av}, defined by the plane of the benzoate phenyl group and the plane composed of a carboxyl group and two Ru atoms (inset figure in Table S2) is relatively small even in **1** and **4** where the steric hindrance according to *o*-F groups is expected (7.4° for **1** and 16.1° for **4**), which is much smaller than the 27.6° observed in $[Ru_2(o\text{-}FPhCO_2)_4(THF)_2]$ that has no such characteristic intramolecular hydrogen bonds.[9] This is probably because the fixing by the hydrogen bonds of $NH_2\cdots F$ somewhat stabilizes such anomalous arrangements. As described above, the shorter Ru−N bond found in all compounds is probably due to the effect of hydrogen bonding.

Synthesis, Characterization, and Structures of 5 and 6. The dithiobiuret Pd and Pt complexes, $[M^{II}(dtb)_2]$ (M = Pd, Pt),[28] which have structural character similar to that of dapy, i.e., the presence of an imino nitrogen atom and two adjacent amine groups, are expected to act as bridgeable CDBBs, i.e., metalloligands.[29] To the best of our knowledge, however, there is no example that exhibits such a bridging mode as M−dtb−M′ (M′ meaning other metal ions). This is because of that the imino nitrogen atom of $[M^{II}(dtb)_2]$ complexes does not have a strong coordination ability.

For assembly reactions with $[M^{II}(dtb)_2]$ (M = Pd, Pt), polar solvents such as THF, DMF, and MeCN are used because the $[M^{II}(dtb)_2]$ complexes are only soluble in polar solvents. Such polar solvents, however, simultaneously act as ligands, consequently competing for coordination at the axial sites of $[Ru_2]$; hence the use of such polar solvents should generally be avoided in assembly reactions with $[Ru_2^{II,II}]$ complexes where possible, as done in previous studies.[1,12−21,27] Nevertheless, the *1-D* chain compounds **5** and **6** were selectively synthesized in high yield in a THF-containing medium from the reaction of $[Ru_2(o\text{-}FPhCO_2)_4(THF)_2]$ and $[M^{II}(dtb)_2]$ in a 1:1 molar ratio. This may be due to the support of hydrogen bonding of $NH_2\cdots O_{eq}$, which must strengthen the N−Ru bond, as is evident in the discrete compounds **1**−**4** (vide infra).

IR spectra of compounds **5** and **6** show two characteristic N−H stretching peaks in the range 3180−3370 cm^{-1}, which are blue-shifted compared to those in $[M^{II}(dtb)_2]$ (3150 and 3310 cm^{-1} for M = Pd and Pt, respectively), whereas the peak positions of C═O stretching vibrations are almost unchanged, proving that the charge distribution remains the same without significant charge transfer between $[Ru_2]$ and the $[M^{II}(dtb)_2]$ unit. Powder reflection spectra of **5** and **6** could be interpreted by a simple summation of respective components (Figure S3). This can be realized by a relationship between the HOMO level of $[Ru_2(o\text{-}FPhCO_2)_4(THF)_2]$ and LUMO level of $[M^{II}(dtb)_2]$ (vide infra).

Compounds **5** and **6** are isostructural in the triclinic $P\bar{1}$ space group. Crystallographic parameters, selected bond lengths and angles, and hydrogen bond distances for **5** and **6** are summarized in Tables S4, S5, and S6, respectively. The formula

dx.doi.org/10.1021/ic401030r | *Inorg. Chem.* 2013, 52, 9908−9914

unit is composed of one $[Ru_2]$ unit and one $[M(dtb)_2]$ unit, each of which has an inversion center on the midpoint of the Ru−Ru bond and Pd (**5**) or Pt (**6**) center, respectively (Z = 1, Figure 3 for **5** and Figure S4 for **6**). The $[M(dtb)_2]$ unit

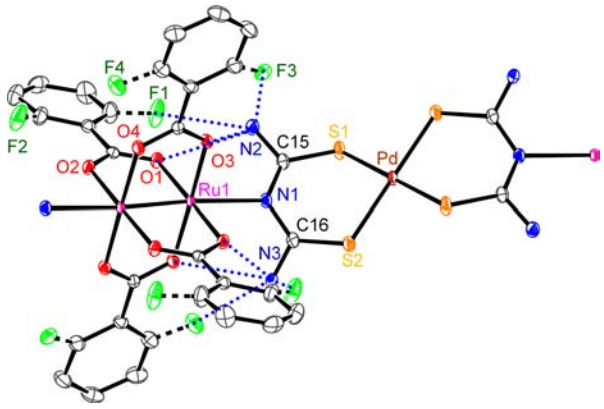

Figure 3. Thermal ellipsoid plot (50% probability) showing the formula unit for **5**, where atoms of N, O, C, F, S, Pd, and Ru are represented in colors of blue, red, gray, green, yellow, brown, and purple, respectively, dashed bonds for the *o*-F atom represent positional disorder, and blue dotted lines represent hydrogen bonds. Hydrogen atoms and crystallization solvents were omitted for clarity.

coordinates to the axial positions of the $[Ru_2]$ unit via the imino nitrogen atom of the dtb ligand with a Ru−N bond length of 2.406(5) and 2.443(3) Å for **5** and **6**, respectively, forming a *1-D* chain motif with a $[-\{Ru_2\}-\{M(dtb)_2\}-]$ repeating unit (Figure 4 for **5** and Figure S5 for **6**). The Ru−

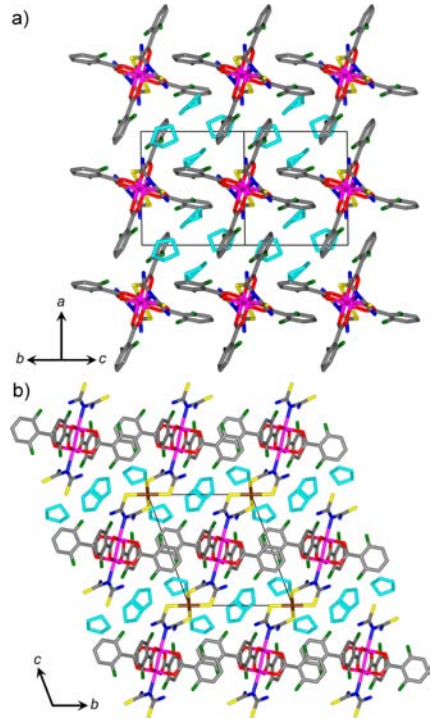

Figure 4. Packing diagram of **5** projected along the [011] direction (a) and the *a* axis (b), where atoms of N, O, C, F, S, Pd, and Ru are represented in colors of blue, red, gray, green, yellow, brown, and purple, respectively, and the THF molecules as crystallization solvents are colored in cyan. Hydrogen atoms were omitted for clarity.

Ru−N angle is almost linear, but the overall feature of the chain is a zigzag with a significant Ru−N···M angle of 145.68(11)° for **5** and 145.74(14)° for **6**. The Ru−Ru distance for **5** and **6** is 2.2835(11) and 2.2894(10) Å, respectively, and the average Ru−O_{eq} (O_{eq} = equatorial oxygen atoms) bond distance is 2.064 and 2.063 Å, respectively, consistent with the $[Ru_2^{II,II}]$ oxidation state.[9] The average M−S distance is 2.2913 Å for **5** with M = Pd and 2.2926 Å for **6** with M = Pt, similar to those in the original $[M^{II}(dtb)_2]$ complexes (2.304 Å for M = Pd and 2.295 Å for M = Pt).[28] The $[M^{II}(dtb)_2]$ unit is not planar because of the presence of large bending and twisting at the bonds of C−S−M, albeit almost flat for the coordination plane around Pd and Pt (i.e., MS_4 plane). As the C15−N1−C16 plane was taken to evaluate the value of ψ, the coordinating dtb ligand does not bisect the paddlewheel arrangement equally, although it nearly does, with ψ = 35.1° and 35.4° for **5** and **6**, respectively, versus the O1−O2−O1*−O2* planes (symmetry operations (*) $-x + 1, -y + 1, -z + 1$). This results in the hydrogen bond formation between one amino group and two oxygen atoms of different carboxylate bridges with N···O distances in the ranges 2.86−3.31 and 2.84−3.32 Å for **5** and **6**, respectively (Figures 3 and S4). The amino group of dtb forms hydrogen bonds with fluorine of the *o*-FPh moiety with N···F distances in the ranges 3.11−3.94 and 3.09−3.98 Å for **5** and **6**, respectively, where the relatively long distances are found for the minor-occupied F atoms in the positional disordering fluorine atoms. The average dihedral angle θ_{av}, defined by the plane of the benzoate phenyl group and the plane composed of a carboxyl group and a diruthenium unit, is 8.6° and 8.8° for **5** and **6**, respectively. These values are very low, as observed in **1** and **4**, even though they apply to the *o*-F benzoate moiety.

The chains run along the ⟨011⟩ direction, where the chains are arranged in an in-phase manner along the ⟨010⟩ direction (the interchain distance corresponds to the length of the *b* axis) and an antiphase manner along the ⟨01−1⟩ direction ($[Ru_2]\cdots M$ = 9.66 Å for **5** and **6**). The intermolecular $\pi-\pi$ interaction, through contacts between phenyl groups of benzoate moieties, exists along the ⟨100⟩ direction (distance between π planes = 3.42 and 3.40 Å for **5** and **6**, respectively). Four THF molecules locate between chains as crystallization solvents, which strongly interact with NH_2 groups of a dtb ligand by hydrogen bonding. The THF molecules are finally released above 340 K (in thermal gravimetric analyses) (Figure S6), followed by a structural decomposition, indicating that the presence of crystallization solvents with hydrogen bonding plays an important role in stabilizing the structures of **5** and **6**.

Consideration of Electronic Structures of 5 and 6. The electronic state of both $[Ru_2(o\text{-}FPhCO_2)_4]$ and $[M(dtb)_2]$ units remains unchanged in **5** and **6**, even though the $[Ru_2^{II,II}]$ unit often functions as an electron donor.[2,14−21] It therefore warrants a mention with regards to the relationship of electronic structures between $[Ru_2(o\text{-}FPhCO_2)_4]$ and $[M(dtb)_2]$ units. We have reported that such charge transfers can be well predicted by evaluating the gap between the HOMO level of donor and the LUMO level of acceptor,[2] and DFT calculation for respective original units (e.g., $[Ru_2(o\text{-}FPhCO_2)_4(THF)_2]$) is useful for obtaining such HOMO/LUMO energy values. In this context, we obtained the frontier orbital energy of $[M^{II}(dtb)_2]$ by DFT calculation. A list of the energy levels of HOMO and LUMO for $[Ru_2(o\text{-}FPhCO_2)_4(THF)_2]$[9] and $[M^{II}(dtb)_2]$ with M = Pd and Pt reported previously[28] is given in Table 1. The LUMO energies of the $[M^{II}(dtb)_2]$ unit are −2.190 and −1.781 eV for M = Pd

dx.doi.org/10.1021/ic401030r | Inorg. Chem. 2013, 52, 9908−9914

Table 1. Estimated Energy Levels (eV) of the HOMO and LUMO of the Related Compounds

compd	HOMO	LUMO
$[Ru_2^{II,II}(o\text{-}FPhCO_2)_4(THF)_2]$	−4.184	−1.724
$[Pd^{II}(dtb)_2]$	−5.854	−2.159
$[Pt^{II}(dtb)_2]$	−5.498	−1.781

and Pt, respectively, which are much higher than the HOMO energy at −4.184 eV calculated for $[Ru_2^{II,II}(o\text{-}FPhCO_2)_4(THF)_2]$, proving the isolated feature of $[Ru_2^{II,II}(o\text{-}FPhCO_2)_4]$ and $[M^{II}(dtb)_2]$ from a viewpoint of charge. This result is in full agreement with the reflection spectra and the magnetic behavior of **5** and **6** (see Supporting Information).

CONCLUSION

Hydrogen-bond-assisted paddlewheel-type $[Ru_2^{II,II}]$ assemblies axially capped by pyridine derivatives for discrete complexes (**1**−**4**) and with planar $[M^{II}(dtb)_2]$ units for *1-D* alternating chains (**5** and **6**), which have seldom been reported to date, were synthesized and structurally characterized. In all cases, the formation of hydrogen bonds between the oxygen atoms of carboxylate and amino groups of the axially coordinating ligand/metalloligand was found, and furthermore, hydrogen bonding as $NH_2\cdots F$ was observed when fluorine is located at the *ortho* position of the benzoate ligand. These hydrogen-bonding forms should strengthen the σ-type coordination bond of Ru−N, i.e., support the complexation of the axial site of $[Ru_2^{II,II}]$. The Ru−N bond length in the present complexes is relatively short compared with similar $[Ru_2^{II,II}]$ complexes reported previously.

Compounds **5** and **6** were selectively synthesized even in THF, which should compete with the building block $[M(dtb)_2]$ for the coordinating sites. Unfortunately, no significant interaction between $[Ru_2]$ and $[M(dtb)_2]$ units or between $[Ru_2]$ units via $[M(dtb)_2]$ as charge transfers and magnetic correlations was observed in **5** and **6** because of the presence of a large energy gap between HOMO of $[Ru_2]$ and LUMO of $[M(dtb)_2]$. Nonetheless, such a dual bonding assembly, supported by hydrogen bonding, is quite an efficient strategy for the design of multidimensional network compounds, such as metal−organic frameworks and porous coordination polymer compounds and functional metal-complex assemblies, with paddlewheel-type dimetal building units.

EXPERIMENTAL SECTION

General Procedures. All synthetic procedures were performed under an inert atmosphere using standard Schlenk-line techniques and a commercial glovebox. All chemicals were purchased from commercial sources and were of reagent grade quality. Solvents were dried using common drying agents and distilled under an ultrapure nitrogen gas before use. The starting materials of $[Ru_2^{II,II}]$ units, $[Ru_2(x\text{-}FPhCO_2)_4(THF)_2]$ (*x*- = *o*-, *m*-, *p*-), were prepared according to the previously reported method.[9] The $[M(dtb)_2]$ complexes with M = Pd, Pt were synthesized according to the literature procedure.[28]

Syntheses of 1 and 2. Compound **1** was synthesized by the following procedure: a solid of 2,6-diaminopyridine (24 mg, 224 mmol) was added to a solution of $[Ru_2(o\text{-}FPhCO_2)_4(THF)_2]$ (50 mg, 56 mmol) in 10 mL of THF. After being stirred for 1 h at room temperature, the pale-brown solution was filtered and separated into 1 mL portions (bottom layer) in narrow diameter glass tubes (ϕ: 8 mm). *n*-Hexane (10 mL) was carefully placed in 1 mL portions on the bottom layer, and the layer was allowed to stand for one week to form **1** as pale-brown block-type crystals. Yield: 33 mg, 89%. Elemental analysis (%) calcd for $C_{38}H_{30}N_6F_4O_8Ru_2$: C, 46.72; H, 3.10; N, 8.60. Found: C, 46.24; H, 3.05; N, 9.32. IR(KBr): ν(C═O), 1550, 1402 cm^{-1}; ν(N−H), 3376 cm^{-1}. Compound **2** was synthesized by the same way as for **1**, where $[Ru_2(m\text{-}FPhCO_2)_4(THF)_2]$ (30 mg, 33 mmol) and 2,6-diaminopyridine (14 mg, 130 mmol) were solved in 5 mL THF. Yield 30 mg, 81%. Elemental analysis (%) calcd for $C_{46}H_{46}N_6F_4O_{10}Ru_2$: C, 49.28; H, 4.14; N, 7.49. Found: C, 49.82; H, 4.58; N, 6.92. IR(KBr): ν(C═O), 1553, 1397 cm^{-1}; ν(N−H), 3476, 3388 cm^{-1}.

Synthesis of 3. A solid of 2,6-diaminopyridine (24 mg, 224 mmol) was added to a solution of $[Ru_2(p\text{-}FPhCO_2)_4(THF)_2]$ (50 mg, 56 mmol) in 15 mL of CH_2Cl_2. After being stirred for 1 h at room temperature, the pale-brown solution was filtered and separated into 1 mL portions (bottom layer) in narrow diameter glass tubes (ϕ: 8 mm). *n*-Hexane (15 mL) was carefully placed in 1 mL portions on the bottom layer, and the layer was allowed to stand for one week to form **3** as pale-brown block-type crystals. Yield: 16 mg, 29%. Elemental analysis (%) calcd for $C_{39}H_{32}N_6Cl_2F_4O_8Ru_2$: C, 43.11; H, 3.03; N, 7.91. Found: C, 42.99; H, 3.07; N, 8.53. IR(KBr): ν(C═O), 1549, 1403 cm^{-1}; ν (N−H), 3479, 3379 cm^{-1}.

Synthesis of 4. A solid of 7-azaindole (22 mg, 200 mmol) was added to a solution of $[Ru_2(o\text{-}FPhCO_2)_4(THF)_2]$ (50 mg, 50 mmol) in 10 mL of CH_2Cl_2. After being stirred for 1 h at room temperature, the pale-brown solution was filtered and separated into 1 mL portions (bottom layer) in narrow diameter glass tubes (ϕ: 8 mm). *n*-Hexane (15 mL) was carefully placed in 1 mL portions on the bottom layer, and the layer was allowed to stand for one week to form **4** as pale-brown block-type crystals. Yield: 36 mg, 65%. Elemental analysis (%) calcd for $C_{42}H_{26}N_4F_4O_8Ru_2$: C, 50.80; H, 2.64; N, 5.64. Found: C, 50.34; H, 3.04; N, 5.39. IR(KBr): ν(C═O), 1551, 1401 cm^{-1}; ν(N−H), 3333 cm^{-1}.

Syntheses of 5 and 6. Compound **5** was synthesized by the following method: a 30 mL THF solution containing a solid of $[Pd^{II}(dtb)_2]$ (21 mg, 50 mmol) was refluxed for 2 h to dissolve the solid completely, and, then, cooled at room temperature. A solid of $[Ru_2(o\text{-}FPhCO_2)_4(THF)_2]$ (50 mg, 50 mmol) was added to this solution and stirred for 1 h at room temperature. After being filtered, the brown solution was placed in a Schlenk tube (bottom layer), which was layered with 60 mL of *n*-hexane (top layer). The layer was left undisturbed for 3 days to form red block-type crystals of **5**. Yield: 28 mg, 41%. Elemental analysis (%) calcd for $C_{40}H_{40}N_6F_4O_{10}PdRu_2S_4$ (**5**·2THF): C, 37.60; H, 3.16; N, 6.58. Found: C, 37.84; H, 3.80; N, 6.59. IR(KBr): ν(C═O), 1549, 1402 cm^{-1}; ν(N−H) 3366, 3187 cm^{-1}. Compound **6** was synthesized by the same method, where $[Pt^{II}(dtb)_2]$ (24 mg, 50 mmol) was used instead of $[Pd^{II}(dtb)_2]$. Yield: 36 mg, 53%. Elemental analysis (%) calcd for $C_{40}H_{40}N_6F_4O_{10}PtRu_2S_4$ (**6**·2THF): C, 35.16; H, 2.95; N, 6.15. Found: C, 35.49; H, 3.04; N, 6.78. IR(KBr): ν(C═O), 1549, 1403 cm^{-1}; ν(N−H) 3331, 3188 cm^{-1}.

Physical Measurements. Infrared spectra were measured on a KBr disk using HORIBA FT-IR 720 (for **1**−**4**) and JASCO FT/IR−4200 (for **5** and **6**) spectrophotometers. Powder reflection spectra were measured on the basis of a reference of $BaSO_4$ using a Shimadzu UV−3150 spectrophotometer with an attachment for reflection spectra. TG-DTA data were conducted on a Shimadzu DTG−60H instrument with a temperature sweep rate of 5 °C/min at a N_2 atmosphere. Magnetic susceptibility measurements were performed using a Quantum Design SQUID magnetometer (MPMS−XL−7T). Direct current measurements were conducted over the temperature range 1.8−300 K and at 0.5 or 0.1 T. The measurements were performed on finely ground polycrystalline samples restrained by Nujol. Diamagnetic contributions were corrected for the sample holder, Nujol, and for the sample using Pascal's constants.[30]

Computational Details. Theoretical ab initio calculations of **1**−**4**, and $[M(dtb)_2]$ with M = Pt and Pd were performed using the density functional theory (DFT) formalism, as implemented in the Gaussian 09 software,[31] with the Beck's three parameter hybrid functional with the correlation functional of Lee, Yang, and Parr (B3LYP).[32] Unrestricted open-shell calculations were performed in the calculations of the molecule containing $[Ru_2]$ units. An effective core potential basis set LanL2TZ with polarization (LanL2TZ(f))[33] for Ru, Pt and

dx.doi.org/10.1021/ic401030r | Inorg. Chem. 2013, 52, 9908−9914

Pd atoms and 6-31G basis sets with polarization and diffuse functions (6-31+G(d))[34] for C, H, F, N, O, and S atoms were adopted. In the calculations, spin polarization with $S_Z = 1$ (triplet spin multiplicity) for $[Ru_2]$ units was used. The atomic coordinates determined by using X-ray crystallography with those for $[M(dtb)_2]$ (M = Pt, Pd) being taken from ref 28 and $[Ru_2(x\text{-}FPhCO_2)_4(THF)_2]$ (*x*- = *o*-, *m*-, *p*-) being taken from ref 9 were used in the calculations of those units.

X-ray Crystallographic Study. Single crystals of **1**−**6** were mounted on a thin Kapton film with Nujol and were cooled to 93(1) or 109(1) K by a stream of cooled N_2 gas. Data collections were carried out on a Rigaku CCD diffractometer (Rigaku Saturn+VariMax or Mercury) with graphite-monochromated Mo Kα radiation (λ = 0.710 70 Å). The structures were solved using direct methods (SIR2008[35]) and expanded using Fourier techniques. The full-matrix least-squares refinement on F^2 was performed on the basis of observed reflections and variable parameters, and the refinement cycle was estimated from unweighted and weighted agreement factors of R1 = $\Sigma||F_o| - |F_c||/\Sigma|F_o|$ ($I > 2.00\sigma(I)$ and all data) and wR2 = $[\Sigma(w(F_o^2 - F_c^2)^2)/\Sigma w(F_o^2)^2]^{1/2}$ (all data). A Sheldrick weighting scheme was used. Neutral atom scattering factors were taken from Cromer and Waber.[36] Anomalous dispersion effects were included in F_c;[37] the values of $\Delta f'$ and $\Delta f''$ were those of Creagh and McAuley.[38] The values for the mass attenuation coefficients are those of Creagh and Hubbell.[39] All calculations were performed using the CrystalStructure crystallographic software package,[40] except for refinement, which was performed using SHELXL-97.[41] The crystallographic data for **1**−**4** and **5** and **6** were summarized in Tables S1 and S4, respectively. The CIF data have been deposited at the Cambridge Data Centre as supplementary publication nos. CCDC−935883, 935879, 935884, 935882, 935880, and 935881 for **1**−**6**, respectively. Copies of the data can be obtained free of charge on application to the CCDC, 12 Union Road, Cambridge CB2 1EZ, U.K. (fax (+44) 1223−336−033; e-mail deposit@ccdc.cam.ac.uk).

■ ASSOCIATED CONTENT

Ⓢ Supporting Information

X-ray crystallographic data in CIF format for **1**−**6**, figures for powder reflection spectra for **1**−**6**, structures for one unit in **1** and **4** and for **6**, TGA profiles for **5** and **6**, magnetic properties of **1**−**6**, and tables associated with crystallography and structural details and magnetic data for **1**−**6**. This material is available free of charge via the Internet at http://pubs.acs.org.

■ AUTHOR INFORMATION

Corresponding Author

*E-mail: miyasaka@imr.tohoku.ac.jp. Phone: +81-22-215-2030. Fax: +81-22-215-2031.

Notes

The authors declare no competing financial interest.

■ ACKNOWLEDGMENTS

This work was supported by a Grant-in-Aid for Scientific Research (No. 21350032; 24245012) and on Innovative Areas ("Coordination Programming" Area 2107, No 24108714) from the Ministry of Education, Culture, Sports, Science, and Technology, Japan, The Sumitomo Foundation, and The Asahi Glass Foundation.

■ REFERENCES

(1) Nozaki, T.; Kosaka, W.; Miyasaka, H. *CrystEngComm* **2012**, *14*, 5398.
(2) Miyasaka, H. *Acc. Chem. Res.* **2013**, *46*, 248.
(3) (a) Charkrabarty, R.; Mukherjee, P. S.; Stang, P. J. *Chem. Rev.* **2011**, *111*, 6810. (b) Cook, T. R.; Zheng, Y.-R.; Stang, P. J. *Chem. Rev.* **2013**, *113*, 734.
(4) Felthouse, T. R. *Prog. Inorg. Chem.* **1982**, *29*, 73.
(5) *Multiple Bonds Between Metal Atoms*, 3rd ed.; Cotton, F. A., Murillo, C. A., Walton, R. A., Eds.; Springer Science and Business Media, Inc.: New York, 2005.
(6) Aquino, M. A. S. *Coord. Chem. Rev.* **2004**, *248*, 1025.
(7) Cotton, F. A.; Walton, R. A. *Multiple Bonds Between Metal Atoms*, 2nd ed.; Oxford University Press: Oxford, 1993.
(8) (a) Kuwabara, M.; Yonemitsu, K. *J. Phys. Chem. Solids* **2001**, *62*, 435. (b) Kuwabara, M.; Yonemitsu, K. *J. Mater. Chem.* **2001**, *11*, 2163. (c) Iguchi, H.; Takaishi, S.; Miyasaka, H.; Yamashita, M.; Matsuzaki, H.; Okamoto, H.; Tanaka, H.; Kuroda, S. *Angew. Chem., Int. Ed.* **2010**, *49*, 552.
(9) Miyasaka, H.; Motokawa, N.; Atsuumi, R.; Kamo, H.; Asai, Y.; Yamashita, M. *Dalton Trans.* **2011**, *40*, 673.
(10) Aquino, M. A. S. *Coord. Chem. Rev.* **1998**, *170*, 141.
(11) Mikuriya, M.; Yoshioka, D.; Hand, M. *Coord. Chem. Rev.* **2006**, *250*, 2194.
(12) Miyasaka, H.; Campos-Fernández, C. S.; Galán-Mascarós, J. R.; Dunbar, K. R. *Inorg. Chem.* **2000**, *39*, 5870.
(13) Motokawa, N.; Oyama, T.; Matsunaga, S.; Miyasaka, H.; Sugimoto, K.; Yamashita, M.; Lopez, N.; Dunbar, K. R. *Dalton Trans.* **2008**, 4099.
(14) Miyasaka, H.; Motokawa, N.; Chiyo, T.; Takemura, M.; Yamashita, M.; Sagayama, H.; Arima, T. *J. Am. Chem. Soc.* **2011**, *133*, 5338.
(15) Miyasaka, H.; Campos-Fernández, C. S.; Clérac, R.; Dunbar, K. R. *Angew. Chem., Int. Ed.* **2000**, *39*, 3831.
(16) Miyasaka, H.; Izawa, T.; Takahashi, N.; Yamashita, M.; Dunbar, K. R. *J. Am. Chem. Soc.* **2006**, *128*, 11358.
(17) Motokawa, N.; Oyama, T.; Matsunaga, S.; Miyasaka, H.; Yamashita, M.; Dunbar, K. R. *CrystEngComm* **2009**, *11*, 2121.
(18) (a) Miyasaka, H.; Motokawa, N.; Matsunaga, S.; Yamashita, M.; Sugimoto, K.; Mori, T.; Dunbar, K. R. *J. Am. Chem. Soc.* **2010**, *132*, 1532. (b) Nakabayashi, K.; Nishio, M.; Kubo, K.; Kosaka, W.; Miyasaka, H. *Dalton Trans.* **2012**, *41*, 6072.
(19) Motokawa, N.; Matsunaga, S.; Takaishi, S.; Miyasaka, H.; Yamashita, M.; Dunbar, K. R. *J. Am. Chem. Soc.* **2010**, *132*, 11943.
(20) (a) Motokawa, N.; Miyasaka, H.; Yamashita, M.; Dunbar, K. R. *Angew. Chem., Int. Ed.* **2008**, *47*, 7760. (b) Motokawa, N.; Miyasaka, H.; Yamashita, M. *Dalton Trans.* **2010**, *39*, 4724.
(21) Miyasaka, H.; Morita, T.; Yamashita, M. *Chem. Commun.* **2011**, *47*, 271.
(22) (a) Rubin, J.; Harmony, T. P.; Sundaralingam, M. *Acta Crystallogr.* **1991**, *C47*, 1712. (b) Crawford, C. A.; Matonic, J. H.; Streib, W. E.; Huffman, J. C.; Dunbar, K. R.; Christou, G. *Inorg. Chem.* **1993**, *32*, 3125.
(23) Kitamura, H.; Ozawa, T.; Jitsukawa, K.; Masuda, H.; Aoyama, Y.; Einaga, H. *Inorg. Chem.* **2000**, *39*, 3294.
(24) Kitamura, H.; Ozawa, T.; Jitsukawa, K.; Masuda, H.; Einaga, H. *Chem. Lett.* **1999**, 1225.
(25) Miyasaka, H.; Clérac, R.; Campos-Fernández, C. S.; Dunbar, K. R. *J. Chem. Soc., Dalton Trans.* **2001**, 858.
(26) Kosaka, W.; Ishii, Y.; Miyasaka, H. *Polyhedron* **2013**, *52*, 1213.
(27) Kosaka, W.; Yamagishi, K.; Yoshida, H.; Matsuda, R.; Kitagawa, S.; Takata, M.; Miyasaka, H. *Chem. Commun.* **2013**, *49*, 1594.
(28) Girling, R. L.; Amma, E. L. *Acta Crystallogr.* **1976**, *B32*, 2903.
(29) Noro, S.; Miyasaka, H.; Kitagawa, S.; Wada, T.; Okubo, T.; Yamashita, M.; Mitani, T. *Inorg. Chem.* **2005**, *44*, 133.
(30) *Theory and Applications of Molecular Paramagnetism*; Boudreaux, E. A., Mulay, L. N., Eds.; John Wiley & Sons: New York, 1976.
(31) Frisch, M. J.; Trucks, G. W.; Schlegel, H. B.; Scuseria, G. E.; Robb, M. A.; Cheeseman, J. R.; Scalmani, G.; Barone, V.; Mennucci, B.; Petersson, G. A.; Nakatsuji, H.; Caricato, M.; Li, X.; Hratchian, H. P.; Izmaylov, A. F.; Bloino, J.; Zheng, G.; Sonnenberg, J. L.; Hada, M.; Ehara, M.; Toyota, K.; Fukuda, R.; Hasegawa, J.; Ishida, M.; Nakajima, T.; Honda, Y.; Kitao, O.; Nakai, H.; Vreven, T.; Montgomery, J. A., Jr.; Peralta, J. E.; Ogliaro, F.; Bearpark, M.; Heyd, J. J.; Brothers, E.; Kudin, K. N.; Staroverov, V. N.; Kobayashi, R.; Normand, J.; Raghavachari, K.; Rendell, A.; Burant, J. C.; Iyengar, S. S.; Tomasi, J.; Cossi, M.; Rega, N.; Millam, J. M.; Klene, M.; Knox, J. E.; Cross, J. B.; Bakken, V.;

Adamo, C.; Jaramillo, J.; Gomperts, R.; Stratmann, R. E.; Yazyev, O.; Austin, A. J.; Cammi, R.; Pomelli, C.; Ochterski, J. W.; Martin, R. L.; Morokuma, K.; Zakrzewski, V. G.; Voth, G. A.; Salvador, P.; Dannenberg, J. J.; Dapprich, S.; Daniels, A. D.; Farkas, Ö.; Foresman, J. B.; Ortiz, J. V.; Cioslowski, J.; Fox, D. J.*Gaussian 09, Revision B.01*; Gaussian, Inc.: Wallingford, CT, 2009.

(32) Becke, A. D. *J. Chem. Phys.* **1993**, *98*, 5648.

(33) (a) Hay, P. J.; Wadt, W. R. *J. Chem. Phys.* **1985**, *82*, 299. (b) Roy, L. E.; Hay, P. J.; Martin, R. L. *J. Chem. Theory Comput.* **2008**, *4*, 1029. (c) Ehlers, A. W.; Böhme, M.; Dapprich, S.; Gobbi, A.; Höllwarth, A.; Jonas, V.; Köhler, K. F.; Stegmann, R.; Veldkamp, A.; Frenking, G. *Chem. Phys. Lett.* **1993**, *208*, 111.

(34) (a) Hariharan, P. C.; Pople, J. A. *Theor. Chim. Acta* **1973**, *28*, 213. (b) Francl, M. M.; Petro, W. J.; Hehre, W. J.; Binkley, J. S.; Gordon, M. S.; DeFrees, D. J.; Pople, J. A. *J. Chem. Phys.* **1982**, *77*, 3654. (c) Clark, T.; Chandrasekhar, J.; Schleyer, P. V. R. *J. Comput. Chem.* **1983**, *4*, 294. (d) Krishnam, R.; Binkley, J. S.; Seeger, R.; Pople, J. A. *J. Chem. Phys.* **1980**, *72*, 650. (e) Gill, P. M. W.; Johnson, B. G.; Pople, J. A.; Frisch, M. J. *Chem. Phys. Lett.* **1992**, *197*, 499.

(35) Burla, M. C.; Caliandro, R.; Camalli, M.; Carrozzini, B.; Cascarano, G. L.; De Caro, L.; Giacovazzo, C.; Polidori, G.; Siliqi, D.; Spagna, R. *J. Appl. Crystallogr.* **2007**, *40*, 609.

(36) Cromer, D. T.; Waber, J. T. *International Tables for Crystallography*; Kynoch Press: Birmingham, U.K., 1974; Vol. *IV*, Table 2.2A.

(37) Ibers, J. A.; Hamilton, W. C. *Acta Crystallogr.* **1964**, *17*, 781.

(38) Creagh, D. C.; McAuley, W. J. *International Tables for Crystallography*; Wilson, A. J. C., Ed.; Kluwer Academic: Boston, MA, 1992; Vol. *C*, Table 4.2.6.8, pp 219−222.

(39) Creagh, D. C.; Hubbell, J. H. *International Tables for Crystallography*; Wilson, A. J. C., Ed.; Kluwer Academic: Boston, MA, 1992; Vol. *C*, Table 4.2.4.3, pp 200−206.

(40) *CrystalStructure 4.0.1: Crystal Structure Analysis Package*; Rigaku Corporation: Tokyo, Japan, 2000−2010.

(41) *SHELX97*: Sheldrick, G. M. *Acta Crystallogr.* **2008**, *A64*, 112.